IOP Conf. Series: Materials Science and Engineering **137** (2016) 012054 doi:10.1088/1757-899X/137/1/012054

The gravity effect on spin coating glucose thin film

P Han and H Wang[1]

Department of Physics, Capital Normal University, Beijing Key Laboratory of Metamaterials and Devices, Key Laboratory of Terahertz Optoelectronics, Ministry of Education, and Beijing Advanced Innovation Center for Imaging Technology, Beijing, 100048, P.R. China

E-mail: wanghai@cnu.edu.cn

Abstract. We demonstrate the gravity effect on spin-coated glucose film by comparing properties of films fabricated by two different methods: erected spin coating (ESC) and inverted spin coating (ISC). A "Bi-Layer" model, *i.e.* substrate effect layer and free layer, for spin coating is proposed to analyze the gravity effect on spin coating process which offers a more accurate prediction on film thickness. The thickness and deposition pattern are different in samples fabricated by ESC and ISC methods in titrating-repeated spin coating experiment. Finally, in a glucose coating/ferromagnetic composite structure, an enhanced Kerr rotation with the enhancement factor of 2.11 is achieved by ISC method.

1. Introduction

Spin coating is an important method for polymer and organic thin films fabrication [1, 2]. In the spin coating process, the liquid is first dropped on the substrate, and then the substrate is accelerated to the designed spinning speed. The solution flows radially outward owing to the action of centrifugal force. However, a small amount is adsorbed on the substrate, and forms film [3, 4]. The first mathematic analysis proposed by Emslie, Bonner and Peck (EBP) that established a model describing the flow characteristics of Newtonian liquid on a rotating substrate [5]. Furthermore, Meyerhofer developed their model by taking the evaporation into account [6]. On the basis of these pioneer works, Bornside *et al.* modified the related parameters on evaporation rate in detail [7, 8]. Subsequent works focused on the exploration of the formation mechanism and properties of films combining liquid flow and evaporation [3, 9, 10].

In all these works, gravity effect on spin coating is neglected traditionally, for the substrate adsorption dominates the formation of thin film under spinning. In the case of erected spin coating (ESC), gravity force and the substrate adsorption are in the same direction in ESC, as shown in Figure 1a. Gravity exerts pressure on liquids and enhances the substrate effect. For the inverted spin coating (ISC), gravity force and the substrate adsorption are in opposite direction, as shown in Figure 1b. In this case, gravity stretches liquids and weakens the substrate adsorption. Therefore, films fabricated by these two methods are different. However, as far as is known, few people uses ISC method, and the differences between ESC and ISC methods have not been investigated in detail [11, 12].

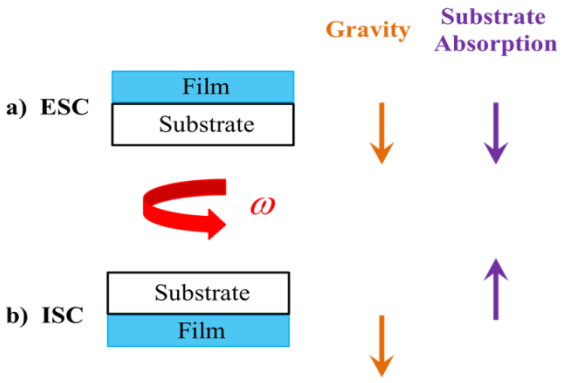

Figure 1. Schematic plot for the experiment, a).for ESC process, the gravity and the substrate adsorption are in the same direction; b). for ISC process, they are in the opposite direction. ω is the spin speed.

Here, we demonstrate that ESC and ISC share same fundamental physics approximately by the similar senses. But the gravity may exert its influences on the film formation resulting in the modifications of microstructures. A titrating-repeated spin coating experiment is performed to demonstrate the differences in the thickness variation with the increase of coating times. To understand the competition between gravity force and substrate adsorption, a "Bi-Layer" model, *i.e.* the substrate effect layer and the free layer, is proposed and applied for our data analysis. Also, we fabricate glucose films on the top of $Ni_{80}Fe_{20}$ substrates which can be used to enhance Kerr rotation of the $Ni_{80}Fe_{20}$ films.

2. Materials and methods

2.1. Experimental procedure

The experiments were performed using a spin coater (Model: WS-650-23NPP) with the maximum spin speed 12000Rpm. Glass substrates of size $25 \times 25\text{mm}^2$ were used for all experiments. The substrates were cleaned by electronic cleaning agent in an ultrasonic bath for ten minutes followed by de-ionized water for five minutes. Dispensed solution (0.5mL) onto the center of the substrate. For ISC, inverted the spin coater immediately after the substrate was fixed on the vacuum chuck. For both methods, the spinning time was sixty seconds. We examined the thicknesses of the full-dried glucose films employing a surface profile tester (Alpha-Step IQ). $Ni_{80}Fe_{20}$ and Fe thin films were deposited using ultra high vacuum magnetron sputtering system (Model: JGP600) with a base pressure 6.3×10^{-5}Pa. The thicknesses were fixed at 100nm ($Ni_{80}Fe_{20}$) and 30nm (Fe) respectively. The deposition rate was 3.18 Å/s ($Ni_{80}Fe_{20}$) and 2.64Å/s (Fe) in experiments. We measured the Kerr rotation θ_K employing the NanoMOKE-III, the longitude MOKE configuration was used. The wavelength of the incident linear polarized light was 660nm, and the incident angle was 45°.

3. "Bi-Layer" model

By the continuity equation of Newtonian liquid, EBP regarded the relationship of film-thinning-rate as a function of processing parameters under the assumption that the centrifugal force equals to viscous force [5]. Furthermore, taking the solvent evaporation during spin coating process into consideration, Meyerhofer revised the relationship between the final film thickness and spin speed assuming that the evaporation rate equals to the viscous flow rate [6]. The relationship between the film thickness h and spin speed ω is $h \propto \omega^{-1/2}$ [3, 4, 6, 7]. Using a mass transfer coefficient to describe vapor-liquid equilibrium process, Bornside *et al.* expressed the evaporation rate with specific parameters [7, 8]. However, some recent works revealed that a bottom-anchored layer formed on the substrate exhibits non-Newtonian behavior due to the substrate effect, which caused a deviation of the index for the spin

speed [4]. Here we simplify the laminar flow model for liquid dynamics as "Bi-layer", *i.e.* the substrate effect layer and the free layer. The substrate effect layer represents the thin liquid layer attached to the substrate that exhibits non-Newtonian nature due to the substrate absorption. The free layer is the liquid layer on the top of the substrate layer. The interaction between the free layer and its "substrate" is the internal interaction in liquid, and therefore the free layer can be considered as the ideal Newtonian liquid. In our model, the film thicknesses of substrate effect layer and free layer are h_1 and h_2 respectively. The total film thickness h_f can be described by:

$$h_f = h_1 + h_2 = m_1\omega^{-\beta_1} + m_2\omega^{-\beta_2} \quad (1)$$

$$m_1 = \left(1 - x_A^0\right)\left[\frac{3\eta_0}{2\rho}\cdot k_1 \cdot \left(x_A^0 - x_{A\infty}\right)\right]^{1/3} \quad (2)$$

$$m_2 = \left(1 - x_A^0\right)\left[\frac{3\eta_0}{2\rho}\cdot k_2 \cdot \left(x_A^0 - x_{A\infty}\right)\right]^{1/3} \quad (3)$$

Here η_0 is the initial viscosity of the coating liquid; ρ is the density of the pure solvent, β_1, and β_2 are the indexes for the spin speed. The evaporation rate for the substrate effect layer and free layer are $k_1 \cdot \left(x_A^0 - x_{A\infty}\right)$ and $k_2 \cdot \left(x_A^0 - x_{A\infty}\right)$ respectively, where k_1 and k_2 are the mass transfer coefficients for the substrate effect layer and the free layer. x_A^0 is the initial concentration of solvent in the coating liquid, $x_{A\infty}$, is the mass fraction of solvent in the overlying gas [7]. The mass transfer coefficients for substrate effect layer and free layer are given by the following expressions:

$$k_1 = \gamma_1 \cdot \frac{1}{\rho} \cdot \frac{P_A M_A}{RT} \quad (4)$$

$$k_2 = \gamma_2 \cdot \frac{1}{\rho} \cdot \frac{P_A M_A}{RT} \quad (5)$$

P_A is the vapor pressure of pure solvent A at temperature T, R is the ideal gas constant, and M_A is the molecular weight of solvent A. γ_1, and γ_2 are parameters for the overlying gas for substrate effect layer and free layer respectively. According to Bornside's work, γ is defined as:

$$\gamma = \frac{cD_g}{\nu_g^{1/2}} \quad (6)$$

The constant c depends on the Schmidt number of the overlying gas. D_g is the binary diffusivity of the solvent in the overlying gas. ν_g is the kinematic viscosity of the overlying gas. All of the parameters and expressions are well defined in the literature.

4. Result and discussion

4.1. Simulation results by "Bi-Layer model" and discussion

Figure 2a demonstrates the film thicknesses h_f as a function of spin speed ω. The solid black line is the fitting results by "Bi-layer" model. As shown in Figure 2a, the film thicknesses of ESC (circle points) and ISC (blue star symbol) series obey the same relationship versus spin speed. We list the fitting parameters in Table 1. The present work estimates the initial viscosity of aqueous glucose solution employing the literature [13].

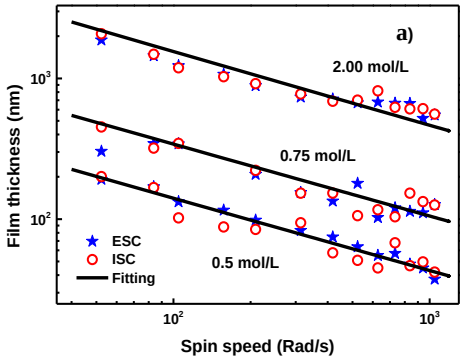

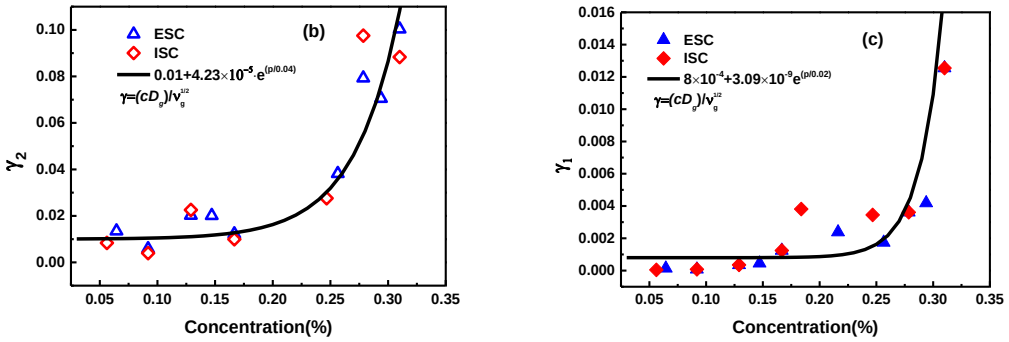

Figure 2. a) The film thickness as a function of spin speed ω, the concentration used is 0.5mol/L, 0.75mol/L, and 2.00mol/L. The blue and red points are the experimental data employing ESC and ISC methods respectively. The solid black lines represent the simulation results by "Bi-Layer model"; (b-c) Relevant parameters γ_2 and γ_1 for overlying gas as a function of the initial concentration of glucose aqueous solution. Erected spin coating and inverted spin coating methods are represented by the blue triangle and the red rhombus respectively. The solid black lines represent the fitting lines, the formula is given in the figure, p is the mass fraction of solute.

β_1 and β_2 are 0.64 and 0.5 respectively, the index for substrate effect layer β_1, deviates from $h_f \propto \omega^{-1/2}$ law due to the non-Newtonian fluid rheology, and the free layer suppresses the evaporation rate. This result is quite similar to the previous works on strong substrate effect, and $\beta_1 = 0.64$ is reasonable in experiments [4]. The latter one, β_2, for free layer term, is consistent with the one in theories for Newtonian liquid, owing to its liquid-to-liquid interface with substrate layer.

Table 1. Constant parameters used for predicting the glucose film thicknesses in Figure 2a.

Parameters for predicted film thickness in Fig.2a, Coating glucose aqueous solution
0.50mol/L-x_A^0-0.908; η_0 =0.0137 Poise;
0.75mol/L-x_A^0-0.871; η_0 =0.0151 Poise;
2.00mol/L-x_A^0-0.690; η_0 =0.0243 Poise;
$x_{A\infty}$=0;
$\rho = 1g/cm^3$;
P_A=0.03128atm;
$M_A = 18g/mol$
$R = 82.06atm \cdot cm^3/mol \cdot K$
$T = 298.15K$

Although substrate effect layer has less contribution on film thickness, its contribution cannot be neglected. Otherwise, the predicted film thickness is smaller than the experimental data as reported in the previous research. And the deviation becomes significant with the increase of concentration [7]. Figure 2b and 2c demonstrate when the mass fraction of solute is less than 20%, γ_2, and γ_1 values are almost constant which consists of previous works [7]. As the mass fraction of solvent is very high, the content of solute can not completely affect the diffusion, the dynamic viscosity of the overlying gas tends to be steady, further lead to the evaporation rate is almost invariant. However, as the mass fraction of solute is greater than 20%, the solute gradually suppress the solvent diffusion with the increase of the mass fraction. The dynamic viscosity of the overlying gas of free layer decreases which causes rapid growth of γ_2 as shown in Figure 2b. With the increase of concentration, γ_1 varies accordingly as shown in Figure 2c. In the case of glass substrate, the adsorption is significant and the

gravity effect on substrate adsorption is ineffective for both ESC and ISC series. Hence, the differences between ESC and ISC is not obvious in our experiments.

Taking viscosity of 1mol/L glucose solution (1.586cP) for the free layer and varying the equivalent viscosity of substrate layer from 0.01 to 100 times than that of the free layer, we can analyze the substrate layer effect on the evolution of film thickness versus spin speed as shown in Figure 3. Compared with the initial mass loss due to centrifugal force at low spin speed the film thickness variation at higher spin speed reflects the liquid spreading process on the substrate as discussed by Meyerhofer. For a comparison, all data are normalized to the thickness obtained at 200rad/s. As shown in Figure 3, with the decrease of equivalent viscosity of the substrate effect layers, the curve gradually tends to flatten up, and the film thinning rate tends to be smaller.

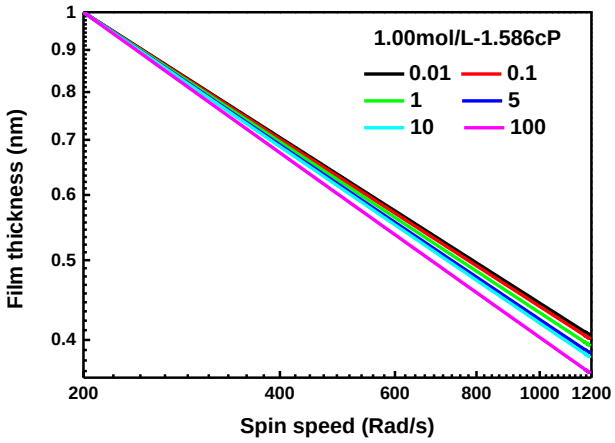

Figure 3. Calculated normalized film thickness versus spin speed using "Bi-Layer" model. Varying the equivalent viscosity ratio of substrate effect layer and free layer ranges from 0.01 to 100: 0.01(black), 0.1(red), 1(green), 5(blue), 10(cyan); 100(magenta). Taking viscosity of 1mol/L glucose solution (1.586cP) for the free layer.

4.2. Titrating-repeated spin coating experiment

We further demonstrate the differences between ESC and ISC through titrating-repeated spin coating method. The initial concentration of aqueous glucose solution is 1.00mol/L; ω is 1046rad/s for each experiment, and the substrates we used was glass. The sample preparation is similar to the above experimental procedure of this work. After drying, we measured the film thicknesses for the first time. Then, another 0.5mL solution was titrated on the surface of dried films for the second time. And the same process was repeated five times for both ESC and ISC methods. Figure 4 shows the relationship between film thickness variation and the number of the experiment.

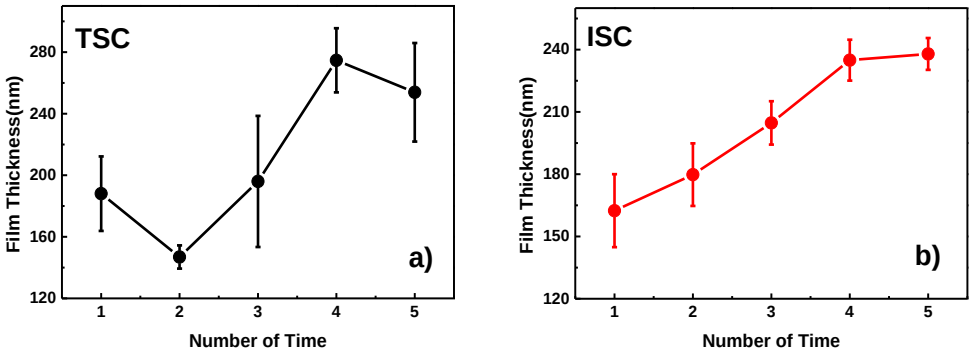

Figure 4. Film thickness versus experimental number: a) ESC method and b) ISC method.

For ESC, as shown in Figure 4a, the film thickness is 188nm after the first spin coating, and then decreases down to 146nm after the second coating and finally rises to 274nm after the fourth spin coating. As shown in previous works, spin-coated thin film is porous after being dried [14, 15]. Therefore, as we titrated liquid on the dried film surface, the liquid fills in the pores under gravity effece. Thus, the thickness of film reduces. Once the internal pores are all filled up, the film thickness rises. However, for ISC, gravity pulls the liquid out from the pores. Hence, the film becomes thicker, as shown in Figure 4b, in which film thickness increases from 163nm to 234nm after the fourth spin coating.

4.3. The gravity effect on deposition patterns

Not only the film thickness but also the deposition patterns may also affected by gravity due to the different kinetic process [16, 17]. We measured the wetting angles of films fabricated by ESC and ISC methods. The initial concentration of aqueous glucose solution is 1.00mol/L, and the spin speed ranged from 209 to 1046rad/s. After drying, another 0.5mL solution was titrated on the surface of dried films and the same drying process was repeated. Finally, a 30nm metal film was deposited on the film surface. Then, we titrated $3\mu L$ of ethanol on the sample surface and measured the wetting angles. Figure 5a and 5b illustrate the results for ESC and ISC respectively. In Figure 5c, the wetting angles are plotted as a function of ω. In this plot, for ESC, the wetting angle reduces from 16.2° to 12.1° with the increase of ω. However, for ISC, with the increase of ω, the wetting angle first decreases from 16.0° to $11.7^{\circ}$and then rises to 16.9°. A minimal value appears when $\omega = 628\text{rad/s}$. In the case of ESC, since gravity and substrate adsorption is in the same direction. The wetting angle reduces monotonically with the increase of ω due to the centrifugal force and substrate adsorption in common sense. However, for ISC, gravity and substrate adsorption are in the opposite direction, the centrifugal force breaks the continuous film at the high spinning rate resulting in a rougher surface morphology under weak substrate adsorption.

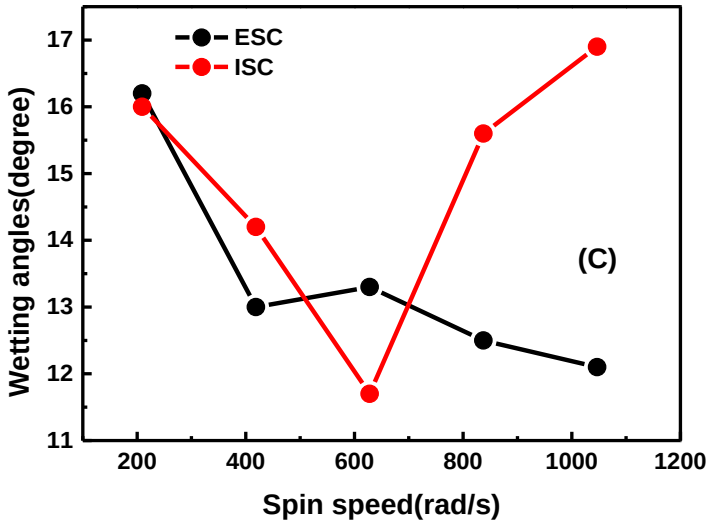

Figure 5. a) The wetting angles. a): ESC method and b): ISC method. c): Wetting angles as a function of spin speed, the black data points correspond to ESC, and the red data points correspond to ISC.

4.4. Application

As an application, we fabricate the glucose film on the top of the $Ni_{80}Fe_{20}$ film. The structure of the glucose film coated on both glass and $Ni_{80}Fe_{20}$ substrates is amorphous as shown in Figure 6a and 6b. The (111) and (200) peaks in Figure 6b are the diffraction peaks of $Ni_{80}Fe_{20}$. As shown in Figure 6c, with the increase of ω, the Kerr rotation rises from 65.75mdeg to 74.78mdeg and then reduces to 34.92mdeg for ESC, the enhancement factor is 1.95. While for ISC, the maximum θ_K is 80.29mdeg, and the enhancement factor is 2.11. The solid line (black) in Figure 6c represents the average Kerr rotation of the bare $Ni_{80}Fe_{20}$ films. The use of dielectric coatings for enhancing the Kerr rotation is a commonly used method [18, 19]. Also, the glucose film fabricated on the top of the $Ni_{80}Fe_{20}$ film equivalent to an organic Fabry-Perot cavity. Linear polarized light propagates within the cavity, which gives rise to multiple reflections off the magnetic layer, the sum of phase and polarization rotation are increased [18, 19].

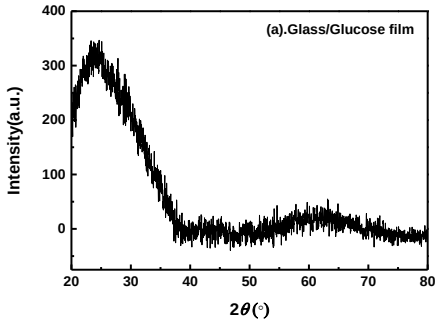

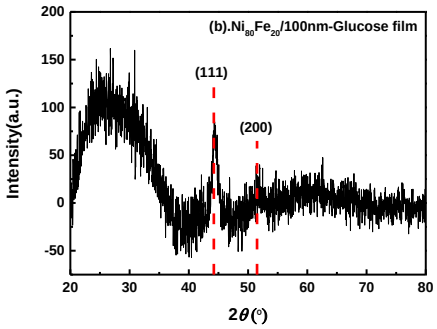

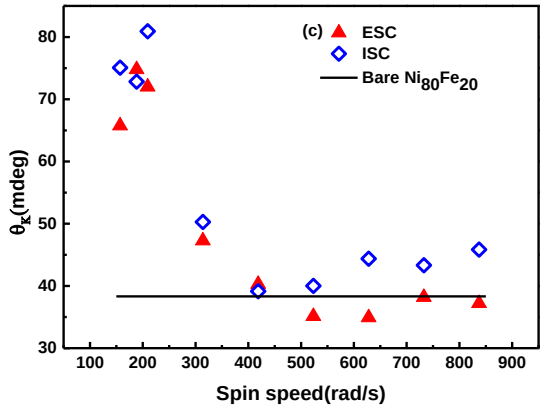

Figure 6. XRD high angle scan in the range $2\theta = 20^{\circ}\sim80^{\circ}$ for glucose film/glass (a) and glucose film/$Ni_{80}Fe_{20}$ film (b). (c). Kerr rotation as a function of spin speed, the glucose film was fabricated employing ESC and ISC method. The concentration of the aqueous glucose solution is 1.00mol/L and the ω ranges from 209.3 to 837.3rad/s. We measure the longitude Kerr rotation of the composite structure including organic films and ferromagnetic materials. The applied magnetic field is 80Oe. The red triangle and blue rhombus symbols represent the Kerr rotation. The solid black line represents the average Kerr rotation of $Ni_{80}Fe_{20}$ films.

5. Summary

In conclusion, we demonstrate the gravity effect on spin coating process through compared the properties of films fabricated employing ESC and ISC methods in detail. ISC shows a unique microcosmic evolution and could be useful for fabrication of films of organic and polymer films. Also, a new "Bi-Layer" model is proposed to understand the spin coating process and simulates the experiment data accurately. Although aqueous glucose solution is selected on purpose in the present work since it is cheap and environmental-friendly, the conclusion has universality.

Acknowledgments

This work was financially supported by the National Natural Science Foundation of China (NSFC) with grant No.11274233 and Beijing education committee under grant KM201610028004.

References

[1] Schmidt R H, Mosbach K and Haupt K 2004 *Adv. Mater.* **8** 719-722
[2] Ikawa M, Yamada T, Matsui H, Minemawari H, Tsutsumi J, Horii Y, Chikamatsu M, Azumi R，Kumai R and Hasegawa T 2012 *Nat. Commun.* **3** 1176
[3] Hall D B, Underhill P and Torkelson J M 1998 *Polym. Eng. Sci.* **38** 2039-2045
[4] Cheung K P, Grover R, Wang Y, Gurkovich C, Wang G and Scheinbeim J 2005 *Appl. Phys. Lett.* **87** 214103
[5] Emslie A G, Bonner F T and Peck L G 1958 *J. Appl. Phys.* **29** 858-862
[6] Meyerhofer D 1978 *J. Appl. Phys.* **49** 3993-3997
[7] Bornside D E, Macosko C W and Scriven L E 1991 *J. Electrochem. Soc.* **38** 317-320
[8] Bornside D E, Brown R A, Ackmann P W, Frank J R, Tryba A A and Geyling F T 1993 *J. Appl. Phys.* **73** 585-600
[9] Birnie D P and Manley M 1996 *Phys. Fluids* **9** 870-875
[10] Mouhamad Y, Mokarian-Tabari P, Clarke N, Jones R A L and Geoghegan M 2014 *J. Appl. Phys.* **116** 123513
[11] Mairaj A K, Curry R J and Hewak D W 2004 *Electron. Lett.* **40** 421
[12] Mairaj A K, Curry R J and Hewak D W 2005 *Appl. Phys. Lett.* **86** 094102
[13] Bui A V and Nguyen M H 2004 *J. Food Eng.* **62** 345-349

[14] Lai J H 1979 *Polym. Eng. Sci.* **19** 1117-1121
[15] Park M S and Kim J K 2004 *Langmuir* **20** 5347-5352
[16] Man X K and Doi M 2016 *Phys. Rev. Lett.* **116** 066101
[17] Bonn D, Eggers J, Indekeu J, Meunier J and Rolley E 2009 *Rev. Mod. Phys.* **81** 739-805
[18] Cantwell P R, Gibson U J, Allwood D A and Macleod H A M 2006 *J. Appl. Phys.* **100** 093901
[19] Qureshi N, Schmidt H and Hawkins A R. 2004 *Appl. Phys. Lett.* **85** 431-433